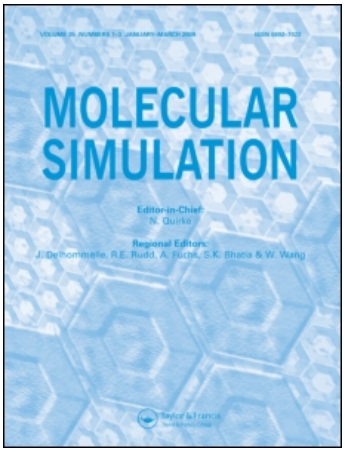

Molecular Simulation
Publication details, including instructions for authors and subscription information:
http://www.informaworld.com/smpp/title~content=t713644482

Free energy landscapes of two model peptides: α-helical and β-hairpin peptides explored with Brownian dynamics simulation

T. Ando[a]; I. Yamato[a]
[a] Department of Biological Science and Technology, Tokyo University of Science, Chiba, Japan

To cite this Article Ando, T. and Yamato, I.(2005) 'Free energy landscapes of two model peptides: α-helical and β-hairpin peptides explored with Brownian dynamics simulation', Molecular Simulation, 31: 10, 683 — 693
To link to this Article: DOI: 10.1080/08927020500183257
URL: http://dx.doi.org/10.1080/08927020500183257

Molecular Simulation, Vol. 31, No. 10, August 2005, 683–693

Taylor & Francis
Taylor & Francis Group

Free energy landscapes of two model peptides: α-helical and β-hairpin peptides explored with Brownian dynamics simulation

T. ANDO* and I. YAMATO

Department of Biological Science and Technology, Tokyo University of Science, 2641 Yamazaki, Noda-shi, Chiba 278-8510, Japan

(Received February 2005; in final form May 2005)

We applied an atomistic Brownian dynamics (BD) simulation with multiple time step method for the folding simulation of a 13-mer α-helical peptide and a 12-mer β-hairpin peptide, giving successful folding simulations. In this model, the driving energy contribution towards folding came from both electrostatic and van der Waals interactions for the α-helical peptide and from van der Waals interactions for the β-hairpin peptide. Although, many non-native structures having the same or lower energy than that of native structure were observed, the folded states formed the most populated cluster when the structures obtained by the BD simulations were subjected to the cluster analysis based on distance-based root mean square deviation of side-chains between different structures. This result indicates that we can predict the native structures from conformations sampled by BD simulation.

Keywords: Protein folding; Brownian dynamics; Free energy landscape; Cluster analysis; Structure prediction

1. Introduction

Understanding the protein folding is often referred to as the second half of genetic code [1]. The prediction of the final folding structure of a protein in terms of physics and chemistry will dramatically affect the various fields ranging from genomic science to nano-technology. Computational efforts have played important roles in this field during the past few decades [2]. With growing computer power and developments of simulation algorithm, molecular dynamics simulations of bigger and more realistic systems are being performed for longer time. However, simulating the folding process of a protein at atomic resolution is still difficult because of the limitation of computational time and the inaccuracy of the force field parameters.

Folding of the key secondary structural elements in proteins, such as α-helix and β-hairpin, has been paid much attention in both experimental and theoretical studies [3–7]. Starting from the basic understanding of the folding process of such key elements, more complex folding process of a protein can be further understood. Experimentally, several peptides that have α-helix or β-hairpin folds have been designed [8–12] and the folding process of such peptides has been studied on the nanosecond time resolution, in which an α-helix and a β-hairpin were demonstrated to fold in a few hundred nanoseconds [4,5] and a few microseconds [6] timescale, respectively. Computationally, those peptides present a more tractable system than proteins. Additionally, new simulation algorithms combined with molecular dynamics simulation, such as multicanonical [13], replica exchange [14], adaptive umbrella sampling [15], distributed computing [16], self-guided molecular dynamics [17] and Tsallis statistics [18], have been developed to overcome the limitations of insufficient sampling. Therefore, folding simulation of such key elements is important not only to understand the basic mechanism of the folding but also to validate the simulation techniques and force fields.

Recently, the folding of α-helices and β-hairpins has been studied by various dynamics simulation algorithms at atomic resolution. The self-guided molecular dynamics method developed by Wu and Wang allowed the simulation of folding process of a 16-residue synthetic helical peptide [17] and a 9-residue β-hairpin peptide [19] in explicit water model within a short simulation time. Schaefer et al. simulated the folding of 13-residue helical

*Corresponding author. Tel.: +81-4-7124-1501. Ext. 4425. Fax: +81-4-7125-1841. Email: tando@rs.noda.tus.ac.jp

Molecular Simulation
ISSN 0892-7022 print/ISSN 1029-0435 online © 2005 Taylor & Francis Group Ltd
http://www.tandf.co.uk/journals
DOI: 10.1080/08927020500183257

and 12-residue β-hairpin peptides with the adaptive umbrella sampling using implicit solvent model [15]. Zagrovic et al. studied folding of a β-hairpin peptide using distributed computing technique [20]. Caflisch and co-workers studied the folding of 15-residue α-helical and 12-residue β-hairpin peptides by molecular dynamics simulations with an implicit solvent model, in which, to observe the folding/unfolding transition, the viscosity of the solvent was not taken into account and simulations was mainly performed at somewhat high temperatures [21]. Replica exchange molecular dynamics (REMD) simulations of α-helix in explicit water solvent were performed by Garcia and Sanbonmatsu and free energy landscapes of the peptides were obtained, in which the importance of backbone shielding by side-chains during α-helix formation was pointed out [22]. REMD of a β-hairpin was also carried out by Garcia and Sanbonmatsu [23] and Zhou et al. [24–26] to obtain the free energy landscape in explicit and implicit solvent models. But in these REMD simulations, native structure was used as the initial configuration. Thus, describing the folding pathways for secondary structure elements at physiological conditions and obtaining the basic information of the folding mechanism from the simulations are still difficult, especially, for the case of β-hairpin formation.

The purpose of the present study was to elucidate the folding mechanism of α-helical and β-hairpin peptides by the long time folding simulations. We have developed an atomistic Brownian dynamics (BD) simulation with multiple time step algorithm and a new implicit solvent model to describe the protein folding process at atomic resolution [27–29]. Using the BD method, the folding mechanism of two peptides was investigated. The first peptide is an analogue of the helical C-peptide of ribonuclease A termed peptide III, whose sequence is acetyl-AETAAAKFLRAHA-NH_2 (13 residues) [30]. From far-UV circular dichroism spectroscopic measurements, peptide III contained about 50% helix in 0.1 M NaCl solution, pH 5.2, 276 K [30]. The second peptide is the designed β-hairpin peptide, BH8, whose sequence is NH_3^+-RGITVNGKTYGR-COO^- (12 residues) [10]. From the NMR and circular dichroism spectrum, this peptide was estimated to adopt a β-hairpin conformation with a two-residue turn at Asn-Gly at 274 K and pH 5 and the β-hairpin population was about 30% [10]. Interstrand residue pairs were Ile3-Tyr10, Val4-Lys9 and Val5-Lys8. We performed folding simulations of both peptides at 298 K, and analyzed the energy landscapes of folding using 20,000 structures obtained from the BD simulations.

2. Methods

2.1 BD Simulation

Folding simulations of peptide III and BH8 from the extended states using the multiple time step BD were performed. The method of multiple time step BD simulation is the same as that described in previous papers except for a slight difference in the potential energy function [27,28]. The differences are described below.

We used the AMBER91 united-atom force field [31] with an angle-dependent, 12–10 hydrogen-bond potential [27]:

$$V_{\mathrm{hb}} = \sum_{i,j}\left(\frac{C_{ij}}{r_{ij}^{12}} - \frac{D_{ij}}{r_{ij}^{10}}\right) F(\theta_{\mathrm{A-H-D}}, \theta_{\mathrm{AA-A-H}}). \quad (1)$$

The angle-dependent term, $F(\theta_{\mathrm{A-H-D}},\theta_{\mathrm{AA-A-H}})$, varies depending on the type of hybridized orbital of the acceptor atom:

For sp^2 acceptor,

$$F(\theta_{\mathrm{A-H-D}}, \theta_{\mathrm{AA-A-H}}) = \cos^4(\theta_{\mathrm{A-H-D}})\cos^4(\theta_{\mathrm{AA-A-H}} - 155^\circ) \quad (\theta_{\mathrm{A-H-D}} > 90^\circ,\ \theta_{\mathrm{AA-A-H}} - 155^\circ > 90^\circ),$$

and for sp^3 acceptor,

$$F(\theta_{\mathrm{A-H-D}},\ \theta_{\mathrm{AA-A-H}}) = \cos^4(\theta_{\mathrm{A-H-D}})\cos^4(\theta_{\mathrm{AA-A-H}} - 109.5^\circ) \quad (\theta_{\mathrm{A-H-D}} > 90^\circ,\ \theta_{\mathrm{AA-A-H}} - 109.5^\circ > 90^\circ), \quad (2)$$

where $\theta_{\mathrm{A-H-D}}$ is the acceptor–hydrogen–donor angle and $\theta_{\mathrm{AA-A-H}}$ is the base–acceptor–hydrogen angle (where the base is the atom that attaches to the acceptor).

To reproduce the solvation effects, three implicit solvent models were used: distance-dependent dielectric (DD) model, solvent-accessible surface area (SA) model, and effective charge (EC) model [29]. In the DD model, $\varepsilon = 2r_{ij}$ was used. The atomic solvation parameters used in the SA model were $\sigma(\mathrm{C}) = 12$ cal/mol/Å^2, $\sigma(\mathrm{O,N}) = -116$ cal/mol/Å^2, $\sigma(\mathrm{S}) = -18$ cal/mol/Å^2 and $\sigma(\mathrm{O^-/N^+}) = -280$ cal/mol/Å^2, which are the same values determined by Wesson and Eisenberg [32] except for the value of $\sigma(\mathrm{O^-/N^+})$. The EC model was introduced by us to represent the shielding effect of oriented water molecules around a point charge [29], in which atomic charge of atom i, q_i, is neutralized as a function of SA of the atom, $\mathrm{SA}_i(\mathbf{r}^N)$:

$$q_i' = q_i\left[\frac{1 - \mathrm{SA}_i(\boldsymbol{r}^N)/S_i}{\alpha_{\mathrm{int}}} + \frac{\mathrm{SA}_i(\boldsymbol{r}^N)/S_i}{\alpha_{\mathrm{ext}}}\right]. \quad (3)$$

Here, q_i' is the effective charge of atom i, S_i is the total solvent-accessible surface area of isolated atom i, α_{int} is a shielding parameter against interior of the solute (wherein α_{int} is set at unity), and α_{ext} is a shielding parameter for exterior water. In this study, $\alpha_{\mathrm{ext}} = 5$ was used.

These parameters used in hydrogen-bond potential and implicit solvent models were optimized manually.

For each peptide, 400 ns BD simulation was performed five times using different random seeds (total simulation time was 2 μs). The initial structures of both peptides were build in extended conformations $(\varphi,\psi) = (-180^\circ,180^\circ)$, followed by steepest descent minimization.

For multiple time step algorithm, short time step, $\Delta\tau$, of 5 fs and long time step, Δt, of 40 fs were used. Simulation temperature was 298 K. Cut-off method was not used.

Coordinates and energies were recorded every 100 ps during the simulation. For analysis, the structures collected for first 10 ns were removed. All calculations were performed on a 2.8 GHz Pentium4 processor based on Linux.

2.2 Distance-based root mean square deviation (dRMS) calculation

Distance-based root mean square deviation is defined as the follow [33,34];

$$\mathrm{dRMS} = \sqrt{\frac{\sum_{n=1}^{N_{\mathrm{pair}}} [d_n(1) - d_n(2)]^2}{N_{\mathrm{pair}}}}, \qquad (4)$$

where $d_n(x)$ is the distance between atoms or geometrical centers of side-chains of pair n in structure x and N_{pair} is the number of pairs considered in this calculation. In this study, distances between geometrical centers of side-chains separated by at least two residues in sequence were considered.

2.3 Cluster analysis

The method of cluster analysis is based on structural similarity similar to the method reported by Daura et al. [35] and Ferrara et al. [21]. The dRMS is evaluated for each pair of structures. For each conformation, the number of neighbors is calculated using a dRMS cutoff of 2 Å. The conformation with the highest number of neighbors (the most populated cluster) is defined as the center of the first cluster. All the neighbors of this conformation are removed from the ensemble of conformations. The center of the second cluster is determined in the same way as for the first cluster. This procedure is repeated until any one structure is assigned to one of such clusters.

2.4 Native contacts

We defined nine backbone–backbone hydrogen bonds (the O···H distance is smaller than 3 Å) between residue i and $i + 4$ as native contacts of peptide III. For BH8, four interstrand backbone–backbone hydrogen bonds (Ile3 NH–Tyr10 CO, Ile3 CO–Tyr10 NH, Val5 NH–Lys8 CO and Val5 CO–Lys8 NH) and three interstrand side-chain–side-chain interactions (Ile3–Tyr10, Thr4–Thr9, and Val5–Lys8; distances between geometrical centers of side-chains are smaller than 7 Å) were used for native contacts. We defined the folded states of peptide III and BH8 by the criterion that the fraction of native contacts $Q \geqq 0.78$ (= 7/9) and $Q \geqq 0.86$ (= 6/7), respectively.

2.5 Free energy calculation and assignment of secondary structure

The free energy of the state at a reaction coordinate q is given by

$$\Delta G(q) = -RT \ln p(q), \qquad (5)$$

where R is the gas constant, T is the temperature and $p(q)$ is the probability of finding the conformation whose reaction coordinate is q.

To assign the secondary structure of the peptide generated by BD simulations, the program DSSP was used [36]. The assignment of a secondary structure to each residue by DSSP is based on hydrogen bond patterns (α-helix, β-bridge, extended β-strand, 3_{10}-helix, π-helix, turn and bend). For calculating the helix content and β-strand content, we divided the number of structured residues that were assigned as α-helix and extended β-strand by the total number of residues, respectively. Since, at least two residues are required for the turn connecting the extended β-strand of β-hairpin, the hairpin content of BH8 was calculated using the following equation [15]: $(N_{\mathrm{ext}} + 2)/N_{\mathrm{res}}$, where N_{ext} is the number of extended β-strand residues given by DSSP and N_{res} is the total number of residues. Because, only six or eight residues with the turn as their center were considered in the estimation of the β-hairpin population of BH8 based on experimental data of NMR and of circular dicroism (CD) [10], we used N_{ext} of 8 in this calculation.

2.6 Folding time

A folding event of peptide III and BH8 was considered as completed when Q reached a value larger than 0.78 (= 7/9) and 0.86 (= 6/7) for the first time.

3. Results

3.1 Folding mechanism, thermodynamics and free energy landscape

Figures 1 and 2 show the fraction of native contacts (Q) and secondary structure contents of the two peptides as a function of simulation time. For peptide III, although there were few states having $Q > 0.8$ due to lack of hydrogen bonds at C-terminus, the peptide reached the folded states

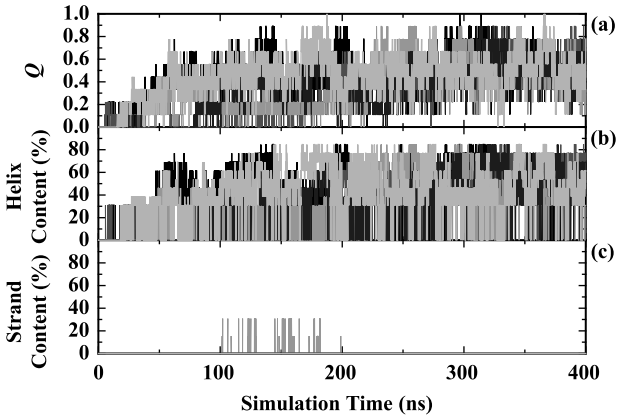

Figure 1. Time evolutions of (a) the fraction of native contacts Q, (b) the helix content and (c) the extended β-strand content during simulations of peptide III. Five trajectories (black, red, green, blue and sky blue) obtained by the BD simulations using different random number seeds are shown.

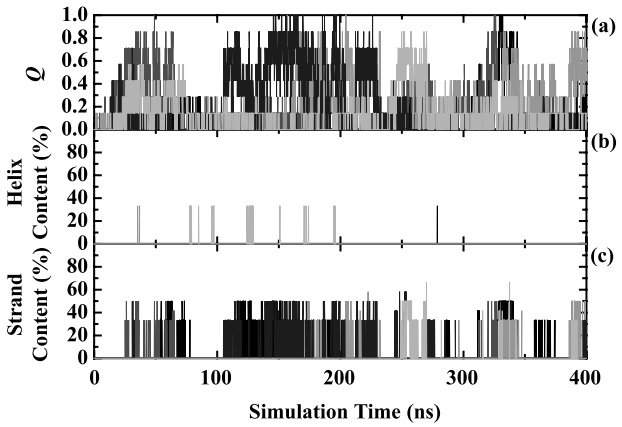

Figure 2. Time evolutions of (a) the fraction of native contacts Q, (b) the helix content and (c) the extended β-strand content during simulations of BH8. Five trajectories (black, red, green, blue and sky blue) obtained by the BD simulations using different random number seeds are shown.

from the extended states within 400 ns in all simulations. Because, the formation of perfect helix ($Q = 1.0$) accompanies with large entropic cost of conformation, this state is not expected to exist in a significant amount. Average helix content and average value of Q, $<Q>$, over five trajectories at 298 K were 36% and 0.38, respectively, which is in excellent agreement with the experimental value of 30% estimated by using circular dicroism spectra at the same temperature (see figure 3b in ref. [30]). For all simulations of peptide III, β-stranded conformation was observed only slightly. In the simulations of BH8, the peptide also folded from the extended structure in all trajectories and significant helix content was not found during the folding processes. Average β-hairpin content and $<Q>$ over five trajectories at 298 K were 6% and 0.15, respectively. Although β-hairpin population of BH8 at room temperature has not been analyzed, β-hairpin content at 274 K was estimated by various methods, where the population of about 30% was calculated by $J_{\mathrm{HN}\alpha}$ values, chemical shifts of NMR spectra and CD spectra, and that of 19% was obtained from NOE data [10]. The NOE intensity is the most sensitive method to estimate a β structure content owing to its inverse dependency with the sixth power of the inter-proton distance [37]. The value of $<Q>$ calculated from our simulation is comparable and in reasonable agreement with the experimental value of NOE. On the other hand, assignment of extended β-strand by DSSP is stringent, while $J_{\mathrm{HN}\alpha}$ values, chemical shifts and CD spectra reflect three dimensional arrangements of peptide bonds and are linear averages over all conformations. Therefore, the β-hairpin content calculated using DSSP (6%) would be underestimated and that calculated with $J_{\mathrm{HN}\alpha}$ values, chemical shifts and CD spectra (30%) would be overestimated, which may be the main reason of the difference of estimation of β-hairpin content. Therefore, we propose that the value calculated from this simulation is not so different from the experimental value.

Figure 3 shows the folding free energy landscape of the peptide III as a function of the number of native backbone–backbone hydrogen bonds and the radius of gyration (R_{g}). The surface was very smooth with one minimum where the peptide was compact with few native hydrogen bonds. The surface was L-shaped. This result indicates that peptide III folding is initiated by non-specific collapse of the chain and then native backbone hydrogen bonds are formed in the compact conformations. Figures 4a and b show the free energy landscapes of the

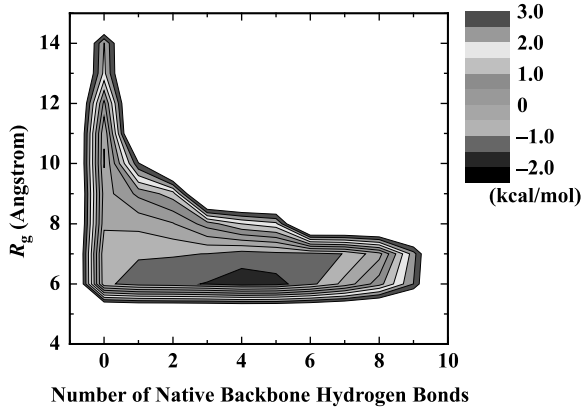

Figure 3. Free energy surface of peptide III at 298 K as functions of the number of native backbone–backbone hydrogen bonds and the radius of gyration (R_{g}) of the peptide.

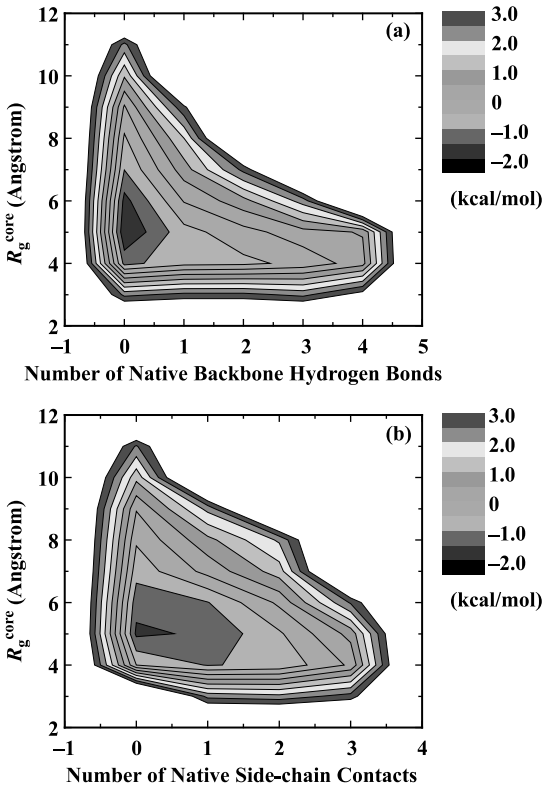

Figure 4. Free energy surface of BH8 at 298 K (a) as functions of the number of native backbone–backbone hydrogen bonds and the radius of gyration of the side-chain atoms; Ile3, Val5, Lys8 and Tyr10 ($R_{\mathrm{g}}^{\mathrm{core}}$) and (b) as functions of the number of native contacts of side-chains and $R_{\mathrm{g}}^{\mathrm{core}}$.

BH8 as functions of the native backbone hydrogen bonds and R_g of the side-chain atoms; Ile3, Val5, Lys8 and Tyr10 (R_g^{core}), and the number of native contacts of side-chains, respectively. Both surfaces were less rugged and contained one minimum where the peptide was compact with few native contacts similar to the case for peptide III. But the shapes of both landscapes were slightly broader than that of peptide III, especially of the surface as functions of native side-chain contacts and R_g^{core}. The landscapes of BH8 indicate that compaction and formation of the native interactions are coupled slightly.

The average effective energy (effective energy is the intra-protein energy plus solvation free energy), its components (van der Waals term, E_{vdW}, electrostatic term screened by DD/EC implicit solvent models, E_{elec} and solvation energy that comes from SA dependent term, E_{SA}), and the free energy of the two peptides as a function of Q are shown in Figures 5a–e and 6a–e. Although, the free energy increased with Q, the total effective energy showed downhill profile for both peptides. The negative gradient of the total effective energy of peptide III was much larger than that of BH8. However, since variances of the total energies were too large, there were many non-native structures having lower effective energy than the energy of the native structure in both systems. This result indicates that it is impossible to predict the native states of the peptides based on the energy alone.

It is well known that the electrostatic contribution of the intra-peptide energy is anti-correlated with that of the solvation free energy. Therefore, effective contribution of the intra-peptide electrostatic energy (E_{elec}') is the electrostatic part of the intra-peptide energy plus that of solvation energy:

$$E'_{elec} = E_{elec} + E_{SA}^{elec} = E_{elec} + E_{SA} - E_{SA}^{non-elec}, \quad (6)$$

where E_{SA}^{elec} and $E_{SA}^{non-elec}$ are the electrostatic and non-electrostatic contribution of solvation energy derived from SA dependent term (E_{SA}), respectively. The average E_{elec}'s as a function of Q calculated by equation (6) are shown in figure 5f for peptide III and figure 6f for BH8, where $E_{SA}^{non-elec}$ were estimated using the solvation parameters, $\sigma(C(sp^3), S) = 10$ cal/mol/Å^2, $\sigma(C(sp^2), C(sp)) = 7$ cal/mol/Å^2 and σ(other atoms) $= 0$ cal/mol/Å^2, which are used in generalized Born/surface area implicit model to represent the non-electrostatic contributions using surface area model [38]. The average values of E_{elec}' of peptide III decreased with Q slightly (figure 5f). On the other hand, the slope of E_{elec}' of BH8 is quite flat. These results indicate that the effective driving energy contributions to the folding of the peptides are

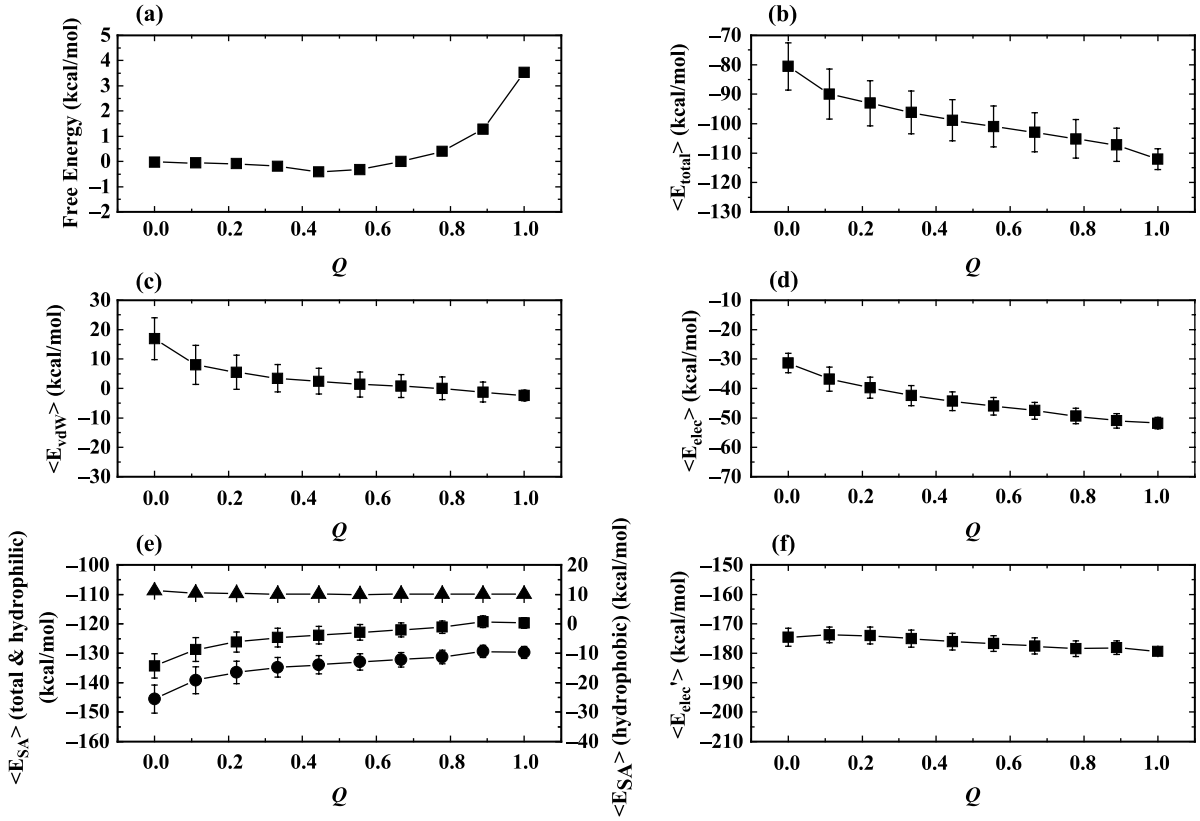

Figure 5. Energy plots of the 2.0×10^4 conformations sampled during five simulations of peptide III at 298 K. (a) Free energy as a function of the fraction of native contacts Q. The free energy was calculated using equation (5) and $p(q)$ was taken as the number of conformations in state q divided by the average value over all states of q. (b) Average effective energy as a function of Q. (c) Average energy of van der Waals term as a function of Q. (d) Average energy of screened electrostatic energy term as a function of Q. (e) Average energy of solvation term derived from solvent-accessible surface dependent terms as a function of Q. Total solvation energy (■), hydrophilic contributions to solvation energy (●) and hydrophobic contributions to solvation energy (▲) are shown. (f) Average effective contribution of the intra-peptide electrostatic energy calculated by equation (6) as a function of Q.

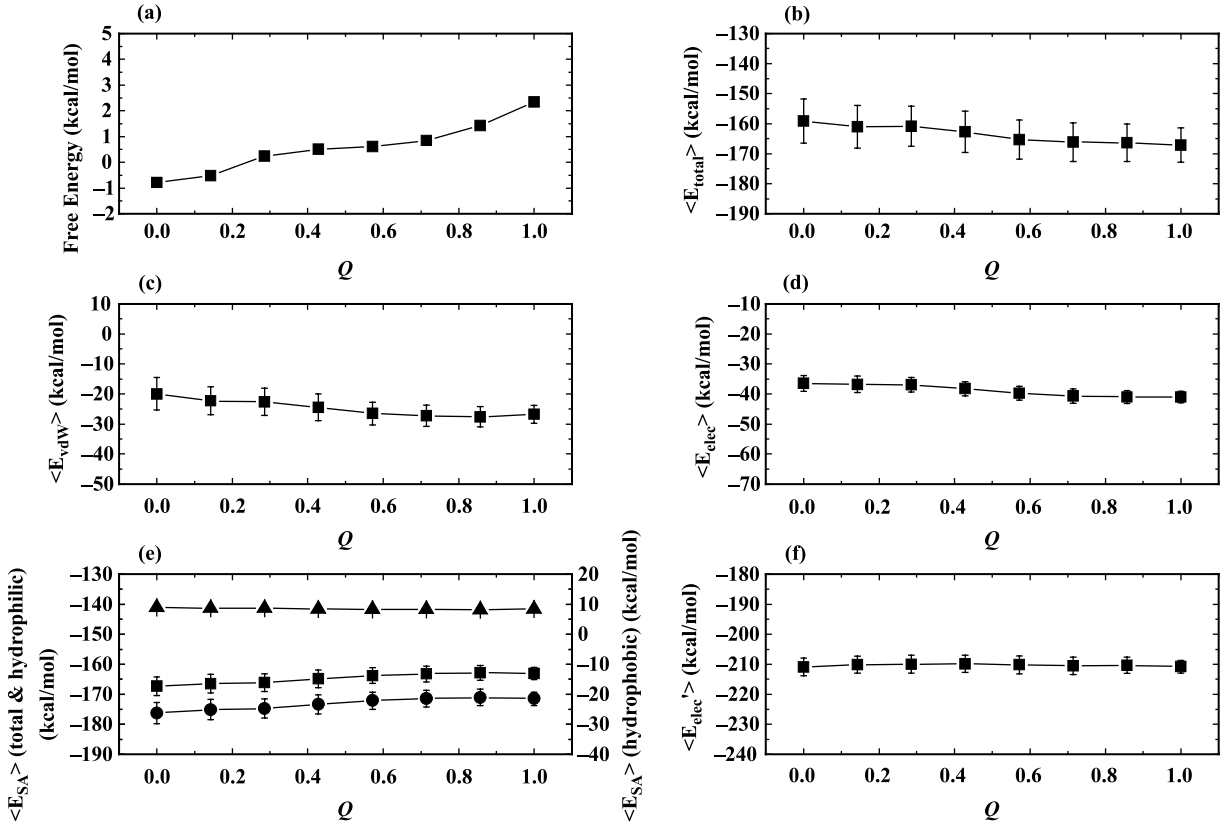

Figure 6. Energy plots of the 2.0×10^4 conformations sampled during five simulations of BH8 at 298 K. (a) Free energy as a function of the fraction of native contacts Q. The free energy was calculated using equation (5) and $p(q)$ was taken as the number of conformations in state q divided by the average value over all states of q. (b) Average effective energy as a function of Q. (c) Average energy of van der Waals term as a function of Q. (d) Average energy of screened electrostatic energy term as a function of Q. (e) Average energy of solvation term derived from solvent-accessible surface dependent terms as a function of Q. Total solvation energy (■), hydrophilic contributions to solvation energy (●) and hydrophobic contributions to solvation energy (▲) are shown. (f) Average effective contribution of the intra-peptide electrostatic energy calculated by equation (6) as a function of Q.

concluded to be derived from both van der Waals and electrostatic terms for the α-helical peptide, peptide III and from van der Waals term for β-hairpin peptide, BH8.

3.2 Cluster analysis

Next, we performed a cluster analysis based on dRMS using about 20,000 structures obtained by the simulations of each peptide. Tables 1 and 2 list average values of energies and the fraction of native contacts Q of the ten most populated clusters of peptide III and BH8, respectively. dRMS's between the structure of the center of cluster 1 and that of other clusters based on geometrical centers of side-chains are also listed in tables 1 and 2. The structures of the centers of the three most populated clusters for both peptides are shown in figure 7. The most populated clusters of peptide III and BH8 contain 7 and 8% of all the conformations, respectively. Interestingly, the most populated cluster had higher average value of Q than that of other clusters and the folded structures belonged to these most populated clusters for both peptides. The central structure of cluster 1 of peptide III had a helical conformation throughout the peptide (figure 7a). For BH8, the central structure of the most populated cluster was a β-hairpin conformation that had side-chains of Ile3, Val5, Lys8 and Tyr10 protruding on the same side of plane of the strands (figure 7b), which is consistent with the NMR data [10].

Most clusters below the second most populated cluster had low average Q values and the central structures of those clusters were disordered ones. The central conformations of the second and third most populated clusters of peptide III were almost helical, but the helical nature of the C-termini of the peptide was disrupted (figure 7c and e). Although, the fourth and fifth most populated clusters of peptide III had average value of Q as high as the first cluster had, these structures were clearly assigned as different clusters from cluster 1. This is due to the difference of side-chain conformations with almost same backbone structures: dRMS based on Cα's between the structures of the centers of cluster 1 and 4 or 5 were 1.1 or 0.4 Å, respectively. An important point is that the cluster analysis makes it possible to predict the native folded states from the structures obtained by the BD simulations.

In this cluster analysis, the distances of geometrical centers of side-chains were used in the calculation of dRMS whose value was the measure of the similarity between pairs of coordinates. When the dRMS calculation based on the distances of Cα's of residues was used, we

Table 1. Average values of energies and the fraction of native contacts Q of the ten most populated clusters of peptide III.

Cluster	*No. of members*	$< E_{total} > $ *	$< E_{vdW} > $ *	$< E_{elec} > $ *	$< E_{SA} > $ *	$<Q>^{\dagger}$	*dRMS(Å)*‡
1	1281	−103.0 ± 7.2	1.1 ± 3.8	−47.9 ± 3.3	−122.1 ± 2.4	0.63 ± 0.15	0.0
2	909	−101.7 ± 6.7	0.4 ± 4.0	−46.6 ± 3.2	−122.4 ± 2.8	0.55 ± 0.15	3.5
3	739	−101.0 ± 6.8	0.2 ± 4.1	−45.7 ± 3.1	−122.6 ± 2.6	0.50 ± 0.12	2.1
4	419	−102.7 ± 6.8	1.7 ± 3.9	−47.9 ± 3.1	−122.0 ± 2.3	0.62 ± 0.14	2.5
5	410	−103.2 ± 7.2	1.1 ± 4.2	−47.6 ± 3.4	−122.0 ± 2.5	0.64 ± 0.13	4.8
6	396	−102.3 ± 6.7	0.4 ± 3.9	−46.5 ± 2.8	−122.7 ± 2.7	0.53 ± 0.12	3.3
7	361	−100.0 ± 7.2	0.7 ± 4.1	−45.0 ± 3.2	−122.7 ± 2.7	0.50 ± 0.12	4.0
8	357	−100.4 ± 7.0	1.6 ± 4.2	−43.6 ± 3.0	−124.8 ± 2.5	0.46 ± 0.11	4.0
9	336	−97.3 ± 6.4	1.5 ± 4.1	−40.5 ± 2.4	−125.3 ± 2.5	0.15 ± 0.06	4.6
10	301	−98.1 ± 6.5	1.8 ± 3.6	−43.3 ± 2.7	−124.1 ± 2.4	0.41 ± 0.11	3.6

* Average values of energies in kcal/mol at 298 K. † Average value of the fraction of native contacts. ‡ dRMS between the structure of the center of cluster 1 and that of other clusters based on geometrical centers of side-chains.

could not distinguish between the structures having the same backbone hydrogen bonds with correct and incorrect interstrand interactions of side-chains (data not shown).

3.3 Kinetics

The folding time was evaluated from the five trajectories of each peptide. The mean folding time at 298 K of peptide III and BH8 were 182 and 175 ns, respectively. Although, the criterion for the folding time is somewhat arbitrary, the estimation for the helical peptide, peptide III, was in good agreement with experimental results on a 21-mer alanine-based peptide [4,5]. On the other hand, the folding time of β-hairpin peptide, BH8, was a few tens times shorter than the experimental result on a 16-mer peptide that corresponds to the C terminus β-hairpin peptide (residue 41–56) of the B1 domain of protein G [6].

4. Discussion

To study the folding mechanism of the key structural elements of proteins, we performed long time simulations of α-helical and β-hairpin peptides at physiological temperature using Brownian dynamics with multiple time step algorithm and implicit solvent DD/SA/EC model from the fully extended conformations. This is the first report of folding simulation of an α-helical and a β-hairpin peptides using a unified force field at constant physiological temperature and of prediction of native structures from the conformations obtained by molecular simulation.

4.1 α-Helical peptide (peptide III)

In the present model, both van der Waals and electrostatic interactions play important roles in helix formation (figure 5). This result is in agreement with the result by Yang and Honig, who found that the major driving force favoring helix formation is van der Waals interactions in the close-packed helix conformation and long range dipole–dipole interactions between peptide groups stabilize helical conformation in poly-alanine peptide [39]. Today, formation and stability of α-helices are well studied compared to β-hairpins, because of the existence of many simple model systems akin to those used for studying α-helix formation. These studies have shown that electrostatic interactions, such as N-cap, C-cap, side-chain–helical dipole electrostatic interactions and side-chain–side-chain electrostatic interactions, stabilize the helical conformation [30,40]. These experimental data are also consistent with our results.

Brooks found that for helical proteins, the folding energy landscapes described in $R_g - Q$ dimensions are more diagonal, suggesting the mechanistic interpretation that local structure formation and native tertiary packing occur

Table 2. Average values of energies and the fraction of native contacts Q of the ten most populated clusters of BH8.

Cluster	*No. of members*	$< E_{total} > $ *	$< E_{vdW} > $ *	$< E_{elec} > $ *	$< E_{SA} > $ *	$<Q>^{\dagger}$	*dRMS(Å)*‡
1	1563	−165.1 ± 6.5	−26.4 ± 3.7	−39.5 ± 2.6	−164.2 ± 2.8	0.53 ± 0.22	0.0
2	1156	−164.2 ± 6.8	−25.4 ± 3.7	−39.0 ± 2.5	−164.2 ± 2.6	0.05 ± 0.07	3.5
3	792	−162.0 ± 6.5	−22.2 ± 4.0	−37.2 ± 2.2	−167.5 ± 2.5	0.05 ± 0.07	2.8
4	707	−164.9 ± 6.3	−24.8 ± 3.4	−39.2 ± 2.4	−164.7 ± 2.4	0.08 ± 0.08	2.9
5	540	−160.8 ± 6.1	−21.7 ± 3.4	−37.0 ± 2.2	−165.7 ± 2.5	0.09 ± 0.07	3.8
6	518	−161.6 ± 6.5	−22.7 ± 3.8	−36.5 ± 2.2	−167.1 ± 2.4	0.08 ± 0.11	2.6
7	423	−165.5 ± 6.6	−28.1 ± 3.7	−39.4 ± 2.6	−162.5 ± 2.9	0.52 ± 0.21	2.0
8	396	−164.8 ± 6.0	−25.4 ± 3.7	−39.5 ± 2.6	−165.2 ± 2.7	0.47 ± 0.25	2.1
8	396	−159.6 ± 6.5	−19.8 ± 3.2	−35.4 ± 2.1	−169.1 ± 2.2	0.18 ± 0.10	2.8
10	308	−158.5 ± 6.4	−17.7 ± 3.4	−35.7 ± 1.9	−169.6 ± 2.1	0.09 ± 0.08	3.3

* Average values of energies in kcal/mol at 298 K. † Average value of the fraction of native contacts. ‡ dRMS between the structure of the center of cluster 1 and that of other clusters based on geometrical centers of side-chains.

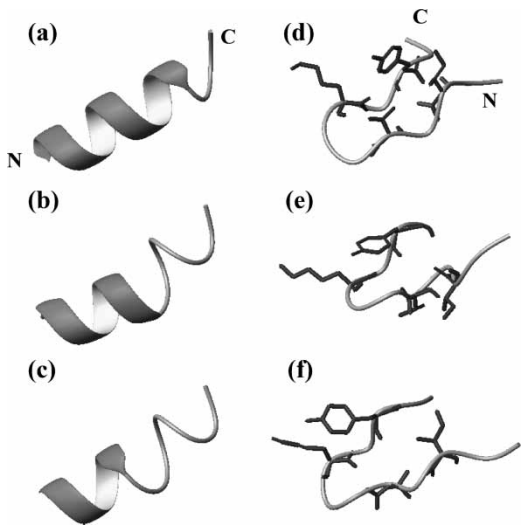

Figure 7. Ribbon representations of the central structures of the three most populated clusters. Left column is for peptide III (a,c,e) and right column is for BH8 (b,d,f). (a and b) The central structures of the most populated clusters, with N and C termini labeled. (c and d) The central structures of the second most populated clusters. (e and f) The central structures of the third most populated clusters. For BH8, residues of Ile3, Val5, Lys8 and Tyr10 are shown in sticks. The figures are generated with MOLMOL [51].

proportionally [41]. In this study, the free energy surface of the helical peptide was L-shaped, suggesting that the folding was initiated by a non-specific collapse (figure 3). This discrepancy may come from the difference between the amino acid sequences and chain lengths of a protein and a peptide. Guo et al. studied folding free energy landscape of a three-helical bundle protein using umbrella sampling method and observed two dominant folding pathways [42]. In one of the pathways, the protein collapsed to an ensemble of compact configurations with less helical content, and then proceeded to the native state through concomitant helix formation and collapse. An alternative pathway suggested the initial formation of significant native helical content before final collapse to the native state. The amino acid sequence of peptide III may prefer the former pathway.

The folding time of helical peptides has been well studied, in which the α-helix formation of a 21-mer alanine based peptide took place in a few hundred nanoseconds time scale [4,5]. In our BD simulation, the mean folding time at 298 K of the helical peptide III was 182 ns, which is in excellent agreement with experimental data of the 21-mer peptide.

4.2 *β*-Hairpin peptide (BH8)

In the present model, van der Waals interactions are the dominant driving force for β-hairpin formation (figure 6). This result is consistent with the estimation of Yang and Honig [43] where they evaluated the energies for various extended conformations of poly-alanine using CHARMM potential function and the finite difference Poisson–Boltzmann method, and the result of Schaefer et al. [15] obtained from the adaptive umbrella sampling simulation of the same peptide with the analytical continuum solvent model. Several studies of β-hairpin peptides have shown that intrastrand hydrophobic interactions play important role in the stability and formation of its structure [44–46]. Mutagenesis analysis of Ile3, Val5, Lys8 and Tyr10 in the BH8 has also shown that interstrand side-chain–side-chain interactions contribute significantly to hairpin stability, in which they thought that alkyl and aromatic groups of those residues made hydrophobic clusters [10]. These experimental observations are also in agreement with our results.

Recently, the free energy landscape of a β-hairpin peptide (the 16-mer C-terminal fragment of protein G) described in $R_g - Q$ dimensions has been explored in explicit and implicit solvent model with various force fields using the replica exchange method and the overall shape was L-shape in all simulations [23–26]. Especially results of Zhou indicated that the folding process was driven by hydrophobic core collapse not by hydrogen bond zipping [24,26]. In the BD model, although the free energy landscape of β-hairpin peptide BH8 was L-shaped, the surface was much broader towards diagonal line (figure 4). The diagonal folding landscape where R_g decreases in parallel with the increase of Q generally provides the mechanistic interpretation that local structure formation and native tertiary packing occur proportionally. Therefore, this broadness towards diagonal line in folding landscape of BH8 indicates that not only hydrophobic collapse but also turn structure (Val5-Asn6-Gly7-Lys8 for BH8) that is formed by only local interactions are important for the folding. This is consistent with the experimental result of Ramirez-Alvarado et al. who showed the importance of the turn stability in hairpin formation by mutagenesis analysis [10].

The lowest free energy state in the free energy landscape of BH8 described in terms of R_g and number of native backbone hydrogen bonds obtained by the BD simulations did not correspond to the native state, but did correspond to the compact configuration without meaningful native hydrogen bonds (figure 4a), which is similar to the "H state" observed in replica exchange molecular dynamics using implicit solvent model with the C-terminus β-hairpin of protein G [25]. On the other hand, higher estimation of native β-hairpin content in free energy landscape of a β-hairpin peptide (66% at 310 K) [24] using explicit solvent model was obtained in contrast to our low content (figure 4). The "H state" obtained [25] was suggested to have resulted from the overestimation of salt-bridge effect between charged residues in implicit solvent model (surface generalized Born implicit solvent model). Thus, Felts et al. [47] improved the implicit solvent model to obtain closer energy landscape to that obtained by explicit solvent model [24]. In the case of BH8 with BD simulation, strong salt-bridges were not observed not only in the compact state without native backbone hydrogen bonds but also in the other regions of energy landscape (data not shown). In this respect, we did not think that the existence of compact state found in our

BD simulations was due to the improper overestimation of salt-bridge effect but that it would be the naturally occurring states in folding towards native structure of BH8. The discrepancy between the landscape shape obtained by replica exchange method and that by long time BD simulations at constant temperature may arise from the difference of the amino acid sequences or of the simulation algorithms and force fields. We need much more study and refinement of force fields and simulation algorithms to elucidate the discrepancy of the energy landscape obtained by implicit and explicit solvent models.

In experiment, kinetics of the folding reaction of 16-mer β-hairpin derived from protein G residue 41–56 has been analyzed by the temperature jump method [6]. Munoz et al. showed that the folding of the hairpin occurred in 6 μs at room temperature, which is about 30 times slower than the rate of α-helix formation of a 21-mer alanine based peptide [4,5]. In our BD simulation, the mean folding time at 298 K of the β-hairpin BH8 was 175 ns, which is much shorter than that of the 16-mer peptide. This discrepancy may be due to the difference of amino acid sequences, especially the turn residues. Theoretical analysis of Munoz et al. suggests that the distance between the hydrophobic cluster of side-chains and the β-turn influences the folding speed strongly [6]. Their model predicts that moving the cluster of hydrophobic amino acids one residue towards the β-turn will speed up the hairpin formation by about fourfold [6]. In BH8, when Ile3, Val5, hydrocarbon part of Lys8 and Tyr10 make hydrophobic cluster, the distance between the side-chain cluster and the β-turn is two residues shorter than that of the 16-mer β-hairpin. Additionally, NMR data have clearly indicated that the 16-mer β-hairpin peptide has a six-residue turn [9], and the sequence in the turn is supposed to have less turn propensity [48]. On the other hand, the turn sequence in the turn of BH8 (Val5–Asn6–Gly7–Lys8) has one of the highest intrinsic preferences for β-turn formation [10,49]. Therefore, the folding time of BH8 could be much faster than that of the 16-mer peptide because not only of the shorter distance between turn and hydrophobic cluster of side-chains but also of the high turn preferences. To solve the discrepancy of folding time, kinetic analysis of BH8 using temperature jump method is necessary.

4.3 General insights

In the present study, we could predict the native structures from the conformations sampled by BD simulation using the cluster analysis based on the distances between side chains for both peptides (tables 1 and 2 and figure 7): native structures were found to form the most populated cluster. On the other hand, free energy minimum of the landscape represented with two order parameters, R_g and Q, corresponded to the state where the peptide was compact with few native contacts for both peptides (figures 3 and 4). Additionally, although average values of native structure content (helical or β-hairpin conformation) of both peptides over five 400 ns simulations were low, especially for BH8, the native structures formed most populated clusters. These results indicate that because the unfolded or non-native conformations are very diverse, it is difficult to characterize these conformations using one or two order parameters such as Q and R_g. Under most experimental conditions, the structure of a peptide will not be highly unique, but there will be an equilibrium distribution between different structures. The experimental data used in structure determination such as NMR correspond to an ensemble and time average over different structures. Therefore, the structure determined by NMR may not necessarily correspond to the free energy minimum described in R_g and Q dimensions. Single molecule experiment with fluorescence resonance energy transfer (FRET) may be useful for obtaining information of such equilibrium distribution.

Principal component analysis was also used to analyze the distribution of conformations [23,50]. But, when principal component analysis was applied to our case, it was not possible to separate the conformations well (data not shown). Therefore, we need other order parameters that can characterize the many conformations more clearly.

5. Conclusions

Using atomistic Brownian dynamics simulation with AMBER force field and three implicit solvent models DD/SA/EC, we simulated the folding of two small peptides, a helical peptide and a β-hairpin peptide, from extended structures with only the knowledge of the primary sequences of the peptides. The advantage of this BD method made it possible to explore the energy landscapes of the peptides and study the folding mechanisms in atomic detail. We showed the driving force towards folding comes from both electrostatic and van der Waals interactions for the α-helical peptide and from van der Waals interactions for the β-hairpin peptide in our model. Also, we could predict the folded states of the peptides from the conformations obtained from BD simulation by using the cluster analysis, not by potential energy information. This result shows that consideration of the entropic component of the free energy can be a crucial factor for peptide structure prediction. The folding simulation of other peptides, especially a protein having more than 50 amino acid residues should be essential for understanding folding mechanism, and this BD simulation method should be useful for such protein folding study.

Acknowledgements

T. Ando acknowledges support from the Academic Frontier Project from MEXT (Ministry of Education, Culture, Sports, Science and Technology of Japan). This

work was supported by a Grant-in-Aid for Scientific Research on Priority Area (C) Genome Information Science from MEXT and by the Open Research Center Project from MEXT to I. Yamato.

References

[1] L.M. Gierasch, J. King. Preface. In *Protein Folding: Deciphering the Second Half of the Genetic Code*, L.M. Gierasch, J. King (Eds.), pp. vii–viii, American Association for the Advancement of Science, Washington DC (1990).

[2] M. Karplus, J.A. McCammon. Molecular dynamics simulations of biomolecules. *Nat. Struct. Biol.*, **9**, 646 (2002).

[3] B.H. Zimm, J.K. Bragg. Theory of the phase transition between helix and random coil in polypeptide chains. *J. Chem. Phys.*, **31**, 526 (1959).

[4] S. Williams, T.P. Causgrove, R. Gilmanshin, K.S. Fang, R.H. Callender, W.H. Woodruff, R.B. Dyer. Fast events in protein folding: helix melting and formation in a small peptide. *Biochemistry*, **35**, 691 (1996).

[5] P.A. Thompson, W.A. Eaton, J. Hofrichter. Laser temperature jump study of the helix ⇔ coil kinetics of an alanine peptide interpreted with a 'kinetic zipper' model. *Biochemistry*, **36**, 9200 (1997).

[6] V. Munoz, P.A. Thompson, J. Hofrichter, W.A. Eaton. Folding dynamics and mechanism of β-hairpin formation. *Nature*, **390**, 196 (1997).

[7] V. Munoz, E.R. Henry, J. Hofrichter, W.A. Eaton. A statistical mechanical model for β-hairpin kinetics. *Proc. Natl. Acad. Sci. USA*, **95**, 5872 (1998).

[8] D.J. Lockhart, P.S. Kim. Internal stark effect measurement of the electric field at the amino terminus of an α-helix. *Science*, **257**, 947 (1992).

[9] F.J. Blanco, G. Rivas, L. Serrano. A short linear peptide that folds into a native stable β-hairpin in aqueous solution. *Nat. Struct. Biol.*, **1**, 584 (1994).

[10] M. Ramirez-Alvarado, F.J. Blanco, L. Serrano. De novo design and structural analysis of a model β-hairpin peptide system. *Nat. Struct. Biol.*, **3**, 604 (1996).

[11] M.S. Searle, D.H. Williams, L.C. Packman. A short linear peptide derived from the N-terminal sequence of ubiquitin folds into a water-stable non-native β-hairpin. *Nat. Struct. Biol.*, **2**, 999 (1995).

[12] A.G. Cochran, N.J. Skelton, M.A. Starovasnik. Tryptophan zippers: stable, monomeric β-hairpins. *Proc. Natl. Acad. Sci. USA*, **98**, 5578 (2001).

[13] U.H.E. Hansmann, Y. Okamoto, F. Eisenmenger. Molecular dynamics, Langevin and hybrid Monte Carlo simulations in a multicanonical ensemble. *Chem. Phys. Lett.*, **259**, 321 (1996).

[14] Y. Sugita, Y. Okamoto. Replica-exchange molecular dynamics method for protein folding. *Chem. Phys. Lett.*, **314**, 141 (1999).

[15] M. Schaefer, C. Bartels, M. Karplus. Solution conformations and thermodynamics of structured peptides: molecular dynamics simulation with an implicit solvation model. *J. Mol. Biol.*, **284**, 835 (1998).

[16] V.S. Pande, I. Baker, J. Chapman, S.P. Elmer, S. Khaliq, S.M. Larson, Y.M. Rhee, M.R. Shirts, C.D. Snow, E.J. Sorin, B. Zagrovic. Atomistic protein folding simulations on the submillisecond time scale using worldwide distributed computing. *Biopolymers*, **68**, 91 (2003).

[17] X. Wu, S. Wang. Self-guided molecular dynamics simulation for efficient conformational search. *J. Phys. Chem. B*, **102**, 7238 (1998).

[18] I. Andricioaei, J.E. Straub. On Monte Carlo and molecular dynamics methods inspired by Tsallis statistics: methodology, optimization, and application to atomic clusters. *J. Chem. Phys.*, **107**, 9117 (1997).

[19] X. Wu, S. Wang, B.R. Brooks. Direct observation of the folding and unfolding of a β-hairpin in explicit water through computer simulation. *J. Am. Chem. Soc.*, **124**, 5282 (2002).

[20] B. Zagrovic, E.J. Sorin, V.S. Pande. β-hairpin folding simulations in atomistic detail using an implicit solvent model. *J. Mol. Biol.*, **313**, 151 (2001).

[21] P. Ferrara, J. Apostolakis, A. Caflisch. Thermodynamics and kinetics of folding of two peptides investigated by molecular dynamics simulations. *J. Phys. Chem. B*, **104**, 5000 (2000).

[22] A.E. Garcia, K.Y. Sanbonmatsu. α-helical stabilization by side chain shielding of backbone hydrogen bonds. *Proc. Natl. Acad. Sci. USA*, **99**, 2782 (2002).

[23] A.E. Garcia, K.Y. Sanbonmatsu. Exploring the energy landscape of a β-hairpin in explicit solvent. *Proteins*, **42**, 345 (2001).

[24] R. Zhou, B.J. Berne, R. Germain. The free energy landscape for β-hairpin folding in explicit water. *Proc. Natl. Acad. Sci. USA*, **98**, 14931 (2001).

[25] R. Zhou, B.J. Berne. Can a continuum solvent model reproduce the free energy landscape of a β-hairpin folding in water? *Proc. Natl. Acad. Sci. USA*, **99**, 12777 (2002).

[26] R. Zhou. Free energy landscape of protein folding in water: explicit vs. implicit solvent. *Proteins*, **53**, 148 (2003).

[27] T. Ando, T. Meguro, I. Yamato. Development of an atomistic Brownian dynamics algorithm with implicit solvent model for long time simulation. *J. Comput. Chem. Jpn*, **1**, 115 (2002).

[28] T. Ando, T. Meguro, I. Yamato. Multiple time step Brownian dynamics for long time simulation of biomolecules. *Mol. Simul.*, **29**, 471 (2003).

[29] T. Ando, T. Meguro, I. Yamato. A new implicit solvent model for Brownian dynamics simulation: solvent-accessible surface area dependent effective charge model. *J. Comput. Chem. Jpn*, **3**, 129 (2004).

[30] K.R. Shoemaker, P.S. Kim, E.J. York, J.M. Stewart, R.L. Baldwin. Tests of the helix dipole model for stabilization of α-helices. *Nature*, **326**, 563 (1987).

[31] S.J. Weiner, P.A. Kollman, D.A. Case, U.C. Singh, C. Ghio, G. Alagona, S.J. Profeta, P. Weiner. A new force field for molecular mechanical simulation of nucleic acids and proteins. *J. Am. Chem. Soc.*, **106**, 765 (1984).

[32] L. Wesson, D. Eisenberg. Atomic solvation parameters applied to molecular dynamics of proteins in solution. *Protein Sci.*, **1**, 227 (1992).

[33] B. Zagrovic, C.D. Snow, S. Khaliq, M.R. Shirts, V.S. Pande. Native-like mean structure in the unfolded ensemble of small proteins. *J. Mol. Biol.*, **323**, 153 (2002).

[34] B. Zagrovic, C.D. Snow, M.R. Shirts, V.S. Pande. Simulation of folding of a small α-helical protein in atomistic detail using worldwide-distributed computing. *J. Mol. Biol.*, **323**, 927 (2002).

[35] X. Daura, W.F. van Gunsteren, A.E. Mark. Folding-unfolding thermodynamics of a β-heptapeptide from equilibrium simulations. *Proteins*, **34**, 269 (1999).

[36] W. Kabsch, C. Sander. Dictionary of protein secondary structure: pattern recognition of hydrogen bonded and geometrical features. *Biopolymers*, **22**, 2577 (1983).

[37] M. Ramirez-Alvarado, T. Kortemme, F.J. Blanco, L. Serrano. β-Hairpin and β-sheet formation in designed linear peptides. *Bioorg. Med. Chem.*, **7**, 93 (1999).

[38] D. Qui, P.S. Shenkin, F.P. Hollinger, W.C. Still. The GB/SA continuum model for solvation. A fast analytical method for the calculation of approximate Born radii. *J. Phys. Chem. A*, **101**, 3005 (1997).

[39] A.S. Yang, B. Honing. Free energy determinants of secondary structure formation: I α-helices. *J. Mol. Biol.*, **252**, 351 (1995).

[40] A.R. Fersht. *Structure and Mechanism in Protein Science*, pp. 523–532, W.H. Freeman and Company, New York (1999).

[41] C.L. Brooks III. Protein and peptide folding explored with molecular simulations. *Acc. Chem. Res.*, **35**, 447 (2002).

[42] Z. Guo, C.L. Brooks III, E.M. Boczko. Exploring the folding free energy surface of a three-helix bundle protein. *Proc. Natl. Acad. Sci. USA*, **94**, 10161 (1997).

[43] A.S. Yang, B. Honig. Free energy determinants of secondary structure formation: II. antiparallel β-sheets. *J. Mol. Biol.*, **252**, 366 (1995).

[44] M.S. Searle, J.M. Griffiths-Jones, H. Skinner-Smith. Energetics of weak interactions in a β-hairpin peptide: electrostatic and hydrophobic contributions to stability from lysine salt bridges. *J. Am. Chem. Soc.*, **121**, 11615 (1999).

[45] S. Honda, N. Kobayashi, E. Munekata. Thermodynamics of a β-hairpin structure: evidence for cooperative formation of folding nucleus. *J. Mol. Biol.*, **295**, 269 (2000).

[46] J.F. Espinosa, V. Munoz, S.H. Gellman. Interplay between hydrophobic cluster and loop propensity in β-hairpin formation. *J. Mol. Biol.*, **306**, 397 (2001).

[47] A.K. Felts, Y. Harano, E. Gallicchio, R.M. Levy. Free energy surfaces of β-hairpin and α-helical peptides generated by replica exchange molecular dynamics with the AGBNP implicit solvent model. *Proteins*, **56**, 310 (2004).

[48] K. Gunasekaran, C. Ramakrishnan, P. Balaram. β-hairpins in proteins revisited: lessons for *de novo* design. *Protein Eng.*, **10**, 1131 (1997).

[49] S.R. Griffiths-Jones, A.J. Maynard, M.S. Searle. Dissecting the stability of a β-hairpin peptide that folds in water: NMR and molecular dynamics analysis of the β-turn and β-strand contributions to folding. *J. Mol. Biol.*, **292**, 1051 (1999).

[50] J. Higo, N. Ito, M. Kuroda, S. Ono, N. Nakajima, H. Nakamura. Energy landscape of a peptide consisting of α-helix, 3_{10}-helix, β-turn, β-hairpin, and other disordered conformations. *Protein Sci.*, **10**, 1160 (2001).

[51] R. Koradi, M. Billeter, K. Wuthrich. MOLMOL: a program for display and analysis of macromolecular structures. *J. Mol. Graphics*, **14**, 51 (1996).